

### Nonseparable Two- and Three-Dimensional Wavelets

Jelena Kovačević and Martin Vetterli

**Abstract**— We present two- and three-dimensional nonseparable wavelets. They are obtained from discrete-time bases by iterating filter banks. We consider three sampling lattices: quincunx, separable by two in two dimensions, and FCO. The design methods are based either on cascade structures or on the McClellan transformation in the quincunx case. We give a few design examples. In particular, the first example of an orthonormal 2-D wavelet basis with symmetries is constructed.

#### I. INTRODUCTION

During the past decade, the field of filter banks, or subband coding, has established itself firmly as one of the very successful methods for compressing signals ranging from speech to images to video [1], [2]. At the same time, and from another field—applied mathematics—the theory of wavelets emerged as a powerful tool for providing time-frequency localized expansions of signals [3]. Recently, it has been shown that the two—filter banks and wavelets—are closely connected, in that one can use iterated filter banks to obtain continuous-time wavelet bases [3]–[5], as well as see filter banks as a “discrete wavelet transform” [6]. While most of these developments concentrated on 1-D signals, and the multidimensional case was handled via the tensor product, some of the more recent efforts concentrated on the “true” multidimensional case, both from the filter bank and the wavelet aspects [7]–[17]. By true we mean that both nonseparable sampling and filtering are allowed. Although the true multidimensional approach suffers from some drawbacks, such as higher computational complexity, it offers a few important advantages. For example, using nonseparable filters leads to more degrees of freedom in design, and consequently better filters. Then, nonseparable sampling opens a possibility of having schemes better adapted to the human visual system. Finally, some previously impossible solutions, such as linear phase and orthonormal filters when the sampling is separable by two in two dimensions, can be achieved using true multidimensional systems.

The main difference when compared to the 1-D treatment is that multidimensional sampling requires the use of lattices. A lattice is the set of all vectors generated by  $\mathbf{D}\mathbf{k}$ ,  $\mathbf{k} \in \mathcal{Z}^n$ , where  $\mathbf{D}$  is the matrix characterizing the sampling process. Note that  $\mathbf{D}$  is not unique for a given sampling pattern. Using the expressions given for sampling rate changes, analysis of multidimensional filter banks (see Fig. 1) can be performed in a similar fashion to their 1-D counterparts. One of the basic tools is the polyphase domain representation, where all signals and filters are decomposed into their polyphase components, each one corresponding to one coset of the sampling lattice. The net result of this process is that, effectively, a single-input single-output periodically time-varying system can be analyzed as if it were a multiple-input multiple-output time-invariant system. The results on alias cancellation and perfect reconstruction are very similar to

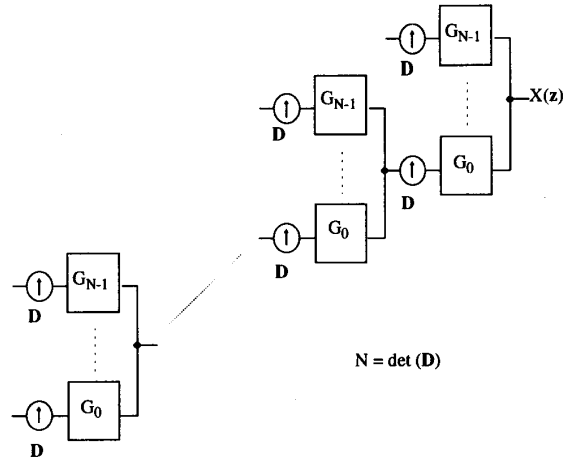


Fig. 1. Analysis/synthesis filter bank with  $N$  branches and sampling by  $\mathbf{D}$ .

their 1-D counterparts [1]. For example, perfect reconstruction with FIR filters is achieved if and only if the determinant of the synthesis (analysis) polyphase matrix is a monomial. On the other hand, to synthesize filter banks we use cascade structures. They are convenient since perfect reconstruction with additional properties such as linear phase can be easily obtained while having low complexity. In the quincunx case, we will also use the McClellan transformation since it has been recognized as a way to build multidimensional filter banks [13], [14] as well as wavelet bases (that is, filter banks that could lead to wavelet bases) [10], [12].

To obtain wavelet bases, we iterate the filter bank as shown in Fig. 2. We identify as  $G_0^{(i)}(\omega)$  the equivalent filter in the low branch after  $i$  steps of filtering and sampling by  $\mathbf{D}$ , where  $G_0^{(0)}(\omega) = 1$ . Now, as in the 1-D case, to make a connection with continuous time, we construct a continuous-time “graphical” function based on the iterated filter  $g_0^{(i)}[\mathbf{k}]$ :  $\varphi^{(i)}(\mathbf{t}) = N^{i/2} g_0^{(i)}[\mathbf{k}]$ ,  $(\mathbf{D}')^i \mathbf{t} \in \mathbf{k} + [0, 1)^n$ , where  $\mathbf{k} = (k_1 \dots k_n)^T$  is an  $n$ -dimensional integer vector and  $\mathbf{t} = (t_1 \dots t_n)^T$ . We are now interested in the limiting behavior of this “graphical” function. The limit of  $\varphi^{(i)}(\mathbf{t})$  exists and is in  $L_2$  if the lowpass filter is regular, and we will call this limit the scaling function  $\varphi(\mathbf{t})$ . By regularity we loosely mean that the obtained scaling function has to have a certain degree of smoothness, that is, following [3], we will try to impose a zero of the highest possible order at all aliasing frequencies [10], [12]. The scaling function satisfies a two-scale equation, that is, it is a linear combination of scaled and shifted versions of itself. Once the scaling function exists, the wavelets can be obtained from

$$\psi_i(\mathbf{t}) = \sqrt{N} \sum_{\mathbf{k} \in \mathcal{Z}^n} g_i[\mathbf{k}] \varphi(\mathbf{D}\mathbf{t} - \mathbf{k}), \quad i = 1, \dots, N - 1 \quad (1)$$

where  $N = \det(\mathbf{D})$ . Note that the coefficients used in the two-scale equation and (1) are the impulse response coefficients of the perfect reconstruction discrete-time filters. The wavelets obtained in such a fashion actually produce an orthonormal basis for  $L_2(\mathcal{R}^n)$  [12]. One more fact that will be needed later is that for the scaling function to exist, the lowpass filter  $g_0[\mathbf{k}]$  has to have at least one zero at all of the aliasing frequencies, that is,  $G_0(\omega = 2\pi(\mathbf{D}')^{-1}\mathbf{k}) = 0$ ,  $\mathbf{k} \in \mathcal{Z}^n$ , where  $2\pi(\mathbf{D}')^{-1}\mathbf{k}$  are the aliasing frequencies. Once a particular

Manuscript received January 12, 1994; revised October 17, 1994. This work was presented at ICASSP 1992 in San Francisco, CA, and ISCAS 1993 in Chicago, IL. This work was supported by the National Science Foundation under grants ECD-88-11111 and MIP 90-14189.

J. Kovačević is with the Signal Processing Research Department, AT&T Bell Laboratories, Murray Hill, NJ, 07974 USA.

M. Vetterli is with the Electrical Engineering and Computer Science Department, University of California at Berkeley, Berkeley, CA, 94720 USA. IEEE Log Number 9410295.

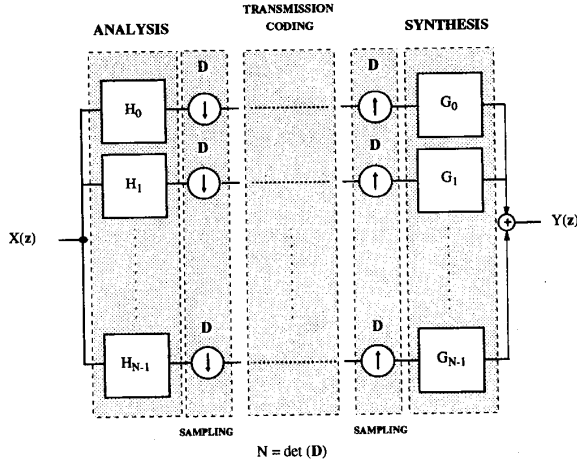


Fig. 2. Filter bank with iterated lowpass branch used for constructing continuous-time wavelet bases.

solution is found, one has to verify that the function to which it converges will be at least continuous. A fast way of estimating it is by monitoring the behavior of the largest first-order differences of the iterates. However, this is only an indicator. In [16], the author develops a method for checking the regularity (actually, continuity) of a 2-D filter. Since the theory behind it is quite involved, here we just outline the process; for more details, the reader is referred to [16]. First, one computes the iterated filter and then finite differences in two directions. This is followed by identifying all polyphase components of these finite differences, and by finding estimates for each one of them. Finally, the maximum of all the above estimates— $\rho$ —is found. Then the lower bound on regularity is  $s = -\log_{\sqrt{N}} \rho$ , [16]. For the solution to be at least continuous,  $s$  has to be positive, that is, we stop the process as soon as  $\rho < 1$ .

## II. QUINCUNX SAMPLING

We will start with the quincunx case, that is, the simplest multidimensional sampling structure that is nonseparable, and will use the following sampling matrix:  $\mathbf{D}_Q = \begin{pmatrix} 1 & 1 \\ 1 & -1 \end{pmatrix}$ . It is called a "symmetry" dilation matrix, used in [12]. Its determinant equals two, and therefore, the corresponding critically sampled filter bank will have two channels. We will now concentrate on design issues. Let us first present a cascade structure that can generate filters being either orthogonal or linear phase. It is obtained by the following:

$$\mathbf{G}_p(z_1, z_2) = \mathbf{R}_0 \cdot \left[ \prod_{i=1}^{K-1} \begin{pmatrix} 1 & 0 \\ 0 & z_i^{-1} \end{pmatrix} \cdot \mathbf{R}_{1_i} \begin{pmatrix} 1 & 0 \\ 0 & z_2^{-1} \end{pmatrix} \mathbf{R}_{2_i} \right]. \quad (2)$$

For the filters to be orthogonal the matrices  $\mathbf{R}_{j_i}$  have to be unitary, while for them to be linear phase matrices have to be symmetric. In the latter case, the filters obtained will have opposite symmetry. Consider, for example, the orthogonal case. Then,  $\mathbf{R} = (1/\sqrt{1+a^2}) \begin{pmatrix} 1 & -a \\ a & 1 \end{pmatrix}$ , and the smallest lowpass filter obtained from the above cascade would be

$$g_0[n_1, n_2] = \frac{1}{\sqrt{(1+a_0^2)(1+a_1^2)(1+a_2^2)}} \cdot \begin{pmatrix} -a_1 & -a_0 a_1 & & \\ -a_2 & -a_0 a_2 & -a_0 & 1 \\ & a_0 a_1 a_2 & -a_1 a_2 & \end{pmatrix}. \quad (3)$$

TABLE I  
TWO SOLUTIONS YIELDING A LOWPASS FILTER  
WITH A THIRD-ORDER ZERO AT  $(\pi, \pi)$

$a_i$	Solution 1	Solution 2
$a_0$	0.18086073	-0.14101995
$a_1$	-0.07356250	0.25065223
$a_2$	-0.35310838	-0.27860678
$a_3$	-0.16178988	-0.23216639
$a_4$	0.19127283	-2.80190711
$a_5$	1.52618074	-0.90189581

TABLE II  
THE SUCCESSIVE LARGEST FIRST-ORDER DIFFERENCES FOR  
THE FILTER OBTAINED USING THE SECOND SOLUTION  
GIVEN IN TABLE I, COMPUTED ON THE RECTANGULAR GRID

Iteration number	Largest first order difference	Rate of convergence
2	1.00396460	
4	0.61660280	1.62822
6	0.35251753	1.74914
8	0.21656604	1.62776
10	0.12829728	1.68800

The highpass filter is obtained by modulation and time-reversal. This filter, with some additional constraints, is the smallest regular 2-D filter, the counterpart of the Daubechies'  $D_2$  filter [3].

We will now show a few design examples. We try to impose a zero of a highest possible order at  $(\pi, \pi)$  on the lowpass filter  $g_0[n_1, n_2]$ , that is,  $(\partial^{k-1} G_0(\omega_1, \omega_2) / \partial \omega_1 \partial^{k-l-1} \omega_2) |_{(\pi, \pi)} = 0$ ,  $k = 1, \dots, m-1$ ,  $l = 0, \dots, k-1$ , and then check its regularity using Villemoes' method [16]. We construct an eight-tap filter by setting  $K = 2$  in (2). After imposing a second-order zero at  $(\pi, \pi)$  on the lowpass filter, the following two solutions  $(a_0, a_1, a_2)$  were found:  $(\mp\sqrt{3}, \mp\sqrt{3}, 2 \pm \sqrt{3})$ , and  $(\pm\sqrt{3}, 0, 2 \pm \sqrt{3})$ . The first solution leads to a regular orthogonal filter, while the second one, interestingly enough, is the same as the well-known Daubechies'  $D_2$  filter [3]. The regularity of the first solution was proven in [16]. This filter is then the smallest regular 2-D filter, a counterpart of  $D_2$ . For larger-size filters, obtaining algebraic solutions becomes a very demanding task. However, numerical approaches are possible. Thus, we set  $K = 4$  and use only  $\mathbf{D}_1 \mathbf{R}_{1_3}$  in the last stage. The filters obtained have 24 taps arranged in six rows (2, 4, 6, 6, 4, 2). After imposing a third-order zero at  $(\pi, \pi)$  on the lowpass filter, two numerical solutions are obtained and are given in Table I. The first-order differences for the second solution in Table I are given in Table II, indicating that the solution will indeed lead to a continuous wavelet basis. To check continuity, we use Villemoes' method as explained earlier. We iterate the filter in even steps on the separable lattice (since the computation is then more efficient), and obtain  $\rho = 0.9601$  in the eighth iteration, which means that the iterated filter will converge to a continuous scaling function. Fig. 4(a) gives the sixth iteration of the lowpass filter.

Another design method is based on the McClellan transformation. Assume we apply the McClellan transformation on the 1-D filter from [18]  $G(z) = (1+z^{-1})^{10} z^{-4} (a+b(z+z^{-1})+c(z+z^{-1})^2+d(z+z^{-1})^3+e(z+z^{-1})^4)$ , where  $a = 0.474823$ ,  $b = -0.654174$ ,  $c = 0.364721$ ,  $d = -0.095712$ ,  $e = 0.01$ , and the filter is given in the form convenient for further transformation. After applying the McClellan transformation a 2-D filter is obtained. Its fourth iteration is given in Fig. 4(b) and the first-order differences given in Table III. Again using Villemoes' method, we obtain very fast convergence

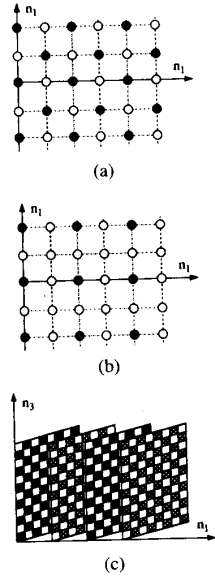


Fig. 3. Three sampling lattices of interest: (a) Quincunx; (b) separable by two in two dimensions; and (c) FCO.

and  $\rho = 0.8929$  in the sixth iteration. Therefore, this iterated filter will produce a continuous scaling function, and consequently, a wavelet basis as well.

### III. SEPARABLE SAMPLING BY TWO IN TWO DIMENSIONS

Let us now examine the system with the sampling lattice as in Fig. 3(b). This lattice is separable, and the sampling matrix is  $\mathbf{D}_s = 2\mathbf{I}$ . The analysis filters are denoted by  $H_0(z_1, z_2), \dots, H_3(z_1, z_2)$ , and they are nonseparable. Their synthesis counterparts are denoted by  $G_0(z_1, z_2), \dots, G_3(z_1, z_2)$ . To obtain perfect reconstruction, we will try for  $\mathbf{G}_p(z_1^2, z_2^2)\mathbf{H}_p(z_1^2, z_2^2) = c \cdot z_1^{-k_1} z_2^{-k_2} \mathbf{I}$ , where the matrices  $\mathbf{H}_p, \mathbf{G}_p$  are the analysis/synthesis polyphase matrices, respectively. We will now see how this can be achieved using a cascade that offers us both orthogonality and linear phase. In [19], a cascade structure was presented generating four linear phase and orthogonal filters of the same size, where two of them are symmetric and two are antisymmetric

$$\mathbf{G}_p(z_1, z_2) = \mathbf{G}_{p0} \prod_{i=1}^k \mathbf{D}(z_1, z_2) \mathbf{U}_i \quad (4)$$

and  $\mathbf{G}_{p0}$  was chosen to be the matrix representing the Walsh-Hadamard transform of size 4,  $\mathbf{D}$  is the diagonal matrix of delays  $(1 \ z_1^{-1} \ z_2^{-1} \ z_1^{-1} z_2^{-1})$ , and  $\mathbf{U}_i$  are scalar persymmetric (that is, they satisfy  $\mathbf{U}_i = \mathbf{J}\mathbf{U}_i\mathbf{J}$ ) unitary matrices. However, it turns out that without simplifications, the above cascade is very difficult to use for constructing wavelets. It has been observed that the number of channels is responsible for the fact that many results look algebraically similar irrespective of the number of dimensions. Thus, we are going to use the factorization of the matrix  $\mathbf{U}_i$  developed for the 1-D case to simplify our cascade [20]. Note first that the matrix  $\mathbf{U}_i$  can be expressed as follows:

$$\mathbf{U}_i = \begin{pmatrix} \mathbf{A}_i & \mathbf{B}_i \\ \mathbf{J}\mathbf{B}_i\mathbf{J} & \mathbf{J}\mathbf{A}_i\mathbf{J} \end{pmatrix} = \mathbf{P} \underbrace{\frac{1}{\sqrt{2}} \begin{pmatrix} \mathbf{I} & \mathbf{I} \\ \mathbf{I} & -\mathbf{I} \end{pmatrix}}_{\mathbf{W}} \underbrace{\begin{pmatrix} \mathbf{r}_{2i} & & & \\ & \mathbf{r}_{2i+1} & & \\ & & \mathbf{r}_{2i} & \\ & & & \mathbf{r}_{2i+1} \end{pmatrix}}_{\mathbf{R}_i} \underbrace{\frac{1}{\sqrt{2}} \begin{pmatrix} \mathbf{I} & \mathbf{I} \\ \mathbf{I} & -\mathbf{I} \end{pmatrix}}_{\mathbf{W}} \mathbf{P}$$

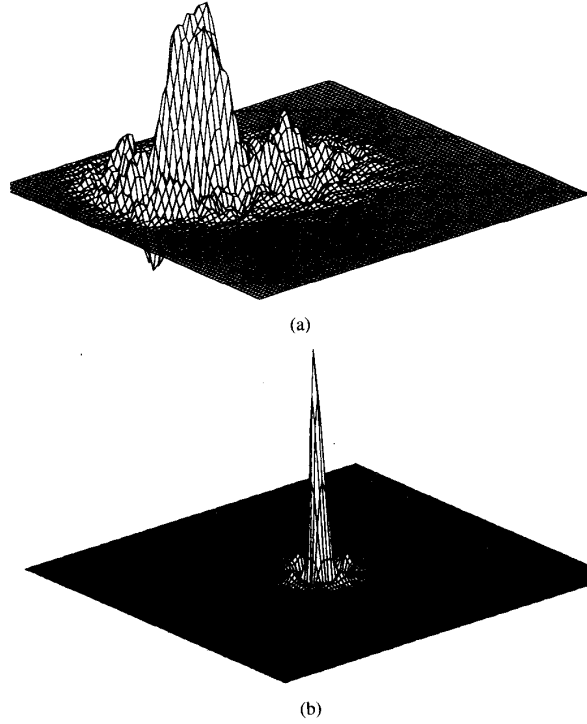


Fig. 4. Quincunx case. (a) Sixth iteration of the regular filter obtained using the second solution given in Table I. (b) Fourth iteration of a regular filter, obtained using the McClellan transformation of the filter given in Section I.

TABLE III  
THE SUCCESSIVE LARGEST FIRST-ORDER DIFFERENCES FOR THE FILTER OBTAINED USING THE MCCLELLAN TRANSFORMATION OF THE LENGTH-19 ONE-DIMENSIONAL FILTER

Iteration number	Largest first order difference	Rate of convergence
2	0.95161612	
4	0.53629625	1.77442
6	0.24966172	2.14809
8	0.10269017	2.43121

where the notation is following [20]. Then for the above matrix to be unitary,  $\mathbf{r}_{2i}$  and  $\mathbf{r}_{2i+1}$  have to be unitary as well, that is, each  $\mathbf{r}_i$  is characterized by one degree of freedom  $\binom{N/2}{2}$  in the general case of  $N$  channels, where  $N$  is even). In addition, the starting matrix  $\mathbf{G}_{p0}$  has to be unitary and satisfy the linear phase testing condition given in [19], and thus  $\mathbf{G}_{p0} = \mathbf{R}_0 \mathbf{W} \mathbf{P}$ . Therefore, the whole structure can be written as

$$\mathbf{G}_p(z_1, z_2) = \mathbf{R}_0 \mathbf{W} \mathbf{P} \prod_{i=1}^k \mathbf{D}(z_1, z_2) \mathbf{P} \mathbf{W} \mathbf{R}_i \mathbf{W} \mathbf{P} \quad (5)$$

where each matrix  $\mathbf{r}_i$  in  $\mathbf{R}_i$  is one Givens rotation  $\mathbf{r}_i = \begin{pmatrix} \cos \alpha_i & -\sin \alpha_i \\ \sin \alpha_i & \cos \alpha_i \end{pmatrix}$ . The filters obtained in this manner are going to be orthogonal, have linear phase, and will be of size  $2(k+1) \times 2(k+1)$ . The number of degrees of freedom will then be  $2(k+1)$ . Note also that, as in [20], the above cascade is valid for all filter banks with an even number of channels.

To construct wavelet bases, we first try to impose one zero at all aliasing frequencies, that is, at  $(z_1, z_2) = (-1, -1)$ ,  $(z_1, z_2) = (1, -1)$ ,  $(z_1, z_2) = (-1, 1)$ . Note that to

obtain filters, one has to upsample the polyphase matrix, that is  $(G_0(z_1, z_2), G_1(z_1, z_2), G_2(z_1, z_2), G_3(z_1, z_2))^T = \mathbf{G}_p(z_1^2, z_2^2)(1, z_1^{-1}, z_2^{-1}, z_1^{-1}, z_2^{-1})^T$ . Thus, for  $z_{1,2} = \pm 1$ , the diagonal matrix of delays in (5),  $\mathbf{D}(z_1, z_2)$ , becomes an identity matrix, and bearing in mind that  $\mathbf{P}^2 = \mathbf{W}^2 = \mathbf{I}$ ,

$$\begin{aligned} \mathbf{G}_p(z_1^2, z_2^2)|_{z_{1,2}=\pm 1} &= \mathbf{R}_0 \mathbf{W} \mathbf{P} \prod_{i=1}^k \mathbf{P} \mathbf{W} \mathbf{R}_i \mathbf{W} \mathbf{P} \\ &= \left( \prod_{i=0}^k \mathbf{R}_i \right) \mathbf{W} \mathbf{P}. \end{aligned} \quad (6)$$

But

$$\begin{aligned} \prod_{i=0}^k \mathbf{R}_i &= \begin{pmatrix} \prod_{i=0}^k \mathbf{r}_{2i} & \\ & \prod_{i=0}^k \mathbf{r}_{2i+1} \end{pmatrix}, \\ \prod_{i=0}^k \mathbf{r}_{2i} &= \begin{pmatrix} \cos \sum_i \alpha_{2i} & -\sin \sum_i \alpha_{2i} \\ \sin \sum_i \alpha_{2i} & \cos \sum_i \alpha_{2i} \end{pmatrix} \end{aligned} \quad (7)$$

and similarly for  $\prod_{i=0}^k \mathbf{r}_{2i+1}$ . Calling  $a_i = \sum_i \alpha_{2i}$  and  $b_i = \sum_i \alpha_{2i+1}$ , we finally obtain

$$\begin{aligned} \mathbf{G}_p^T(z_1^2, z_2^2)|_{z_{1,2}=\pm 1} &= \begin{pmatrix} \cos a_i & \sin a_i & \sin a_i & \cos a_i \\ -\sin a_i & \cos a_i & \cos a_i & -\sin a_i \\ \cos b_i & \sin b_i & -\sin b_i & -\cos b_i \\ -\sin b_i & \cos b_i & -\cos b_i & \sin b_i \end{pmatrix}. \end{aligned}$$

Now the condition that  $G_0(-1, -1) = 0$  translates to  $\cos a_i = \sin a_i$ . Bearing also in mind that  $G_0(1, 1) = 2$  [12], we get that

$$a_i = \sum_i \alpha_{2i} = 2n\pi + \frac{\pi}{4} \quad (8)$$

that is, the sum of all even angles has to equal  $2n\pi + \pi/4$ . In a similar manner, we get that  $G_0(1, -1) = G_0(-1, 1) = 0$  by construction. Thus, it is sufficient for the sum of all even angles to satisfy (8), and the lowpass filter will have a zero at all three aliasing frequencies. This is similar to the condition in the 1-D two-channel case, where the sum of all angles has to be  $\pi/4$  [21].

Having presented a cascade structurally producing filters being both orthogonal and linear phase, let us now give a design example leading to a continuous-time orthonormal wavelet basis characterized by a scaling function  $\varphi(t_1, t_2)$  and three "mother" wavelets  $\psi_i(t_1, t_2)$ ,  $i = 1, 2, 3$ , where both the scaling function and the wavelets are symmetric/antisymmetric. We start by using (5) with  $k = 2$  leading to filters of size  $6 \times 6$ , and requiring the lowpass filter to have a second-order zero at all three aliasing frequencies, that is  $G_0(z_1, z_2) = 0$ ,  $\partial G_0(z_1, z_2)/\partial z_{1,2} = 0$ , for  $(z_1, z_2) = (-1, -1)$ ,  $(z_1, z_2) = (1, -1)$ ,  $(z_1, z_2) = (-1, 1)$ . Upon solving the set of nonlinear equations, one gets the following solution:

$$\begin{aligned} \alpha_0 &= \frac{\pi}{4}, & \alpha_1 &= \pi - \arcsin \frac{1}{4}, \\ \alpha_2 &= 0, & \alpha_3 &= 2 \arcsin \frac{1}{4} - \pi, \\ \alpha_4 &= 0, & \alpha_5 &= -\frac{\pi}{2} - \arcsin \frac{1}{4}. \end{aligned} \quad (9)$$

It is obvious from the above that the even angles indeed sum up to  $\pi/4$  as required by (8). As we said before, now we have to check the regularity of the obtained solution. For this solution, the maximum first-order differences decrease with an almost constant rate, but this is only an indicator, and we will use the method from [16]. The lower

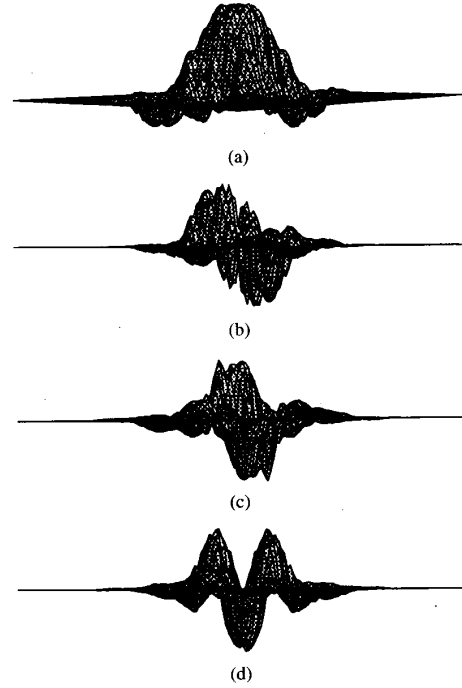


Fig. 5. Fourth iteration of the scaling function (a) and wavelets ((b)=wavelet 1, (c)=wavelet 2, (d)=wavelet 3) obtained using cascade (5) with  $k = 2$  and angles as in (9).

bound on regularity in our case is found in iteration six and equals to  $s = 0.2006$  which tells us that the function is at least continuous. The fourth iteration of the scaling function and the corresponding wavelets are given in Fig. 5 (frontal view is given so as to make the symmetries obvious).

#### IV. FCO SAMPLING

In three dimensions, one can follow the same approach as before. Thus, for the FCO sampling case (nonseparable sampling by two in three dimensions) and matrix

$$\mathbf{D}_{FCO} = \begin{pmatrix} 1 & 0 & 1 \\ -1 & -1 & 1 \\ 0 & -1 & 0 \end{pmatrix}$$

with  $\mathbf{D}_{FCO}^3 = 2\mathbf{I}$ , the following cascade is used:  $\mathbf{G}_p(z_1, z_2, z_3) = \mathbf{R}_0 \cdot \mathbf{D}_1 \mathbf{R}_1 \mathbf{D}_2 \mathbf{R}_2 \mathbf{D}_3 \mathbf{R}_3$  with the same notation as before. Imposing a second-order zero at  $(\pi, \pi, \pi)$  leads to one of the possible solutions as follows:  $a_0 = -a_1 = -2 - \sqrt{3}$ ,  $a_2 = -2 + \sqrt{3}$ ,  $a_3 = \sqrt{3}$ . Setting  $a_2 = -a_1$ , a different set of solutions is obtained,  $a_1 = \pm\sqrt{7} \pm 4\sqrt{3}$ , where four combinations are possible, and  $a_0 = (-4 + 13a_1 - a_1^3)/2$ ,  $a_3 = a_1(3 - 2\sqrt{3})$ . Another useful cascade is given in [12], which allows construction of an  $n$ -dimensional linear phase solution from the  $(n-1)$ -dimensional one, for the two-channel nonseparable case. A useful feature of this cascade is that the smallest size filters (the first block in the cascade) are a general solution (which is usually not the case with multidimensional solutions due to the fact that factorization theorems are lacking). Based on this cascade, highly regular synthesis filters can be constructed as has been already observed in [10], [12] for 2-D diamond shaped filters, as was shown in Section I. In [22], a three-dimensional perfect reconstruction linear phase filter pair is constructed using the above cascade and is used for processing of digital video. In three dimensions, highly regular filters

are obtained by convolving the following filter:  $G_0(z_1, z_2, z_3) = 6 + z_1 + z_1^{-1} + z_2 + z_2^{-1} + z_3 + z_3^{-1}$ , a number of times with itself.

#### ACKNOWLEDGMENT

The authors would like to thank Dr. Villemoes for his help in determining the regularity of the filters, as well as for the software he supplied. We also thank anonymous reviewers for their valuable comments.

#### REFERENCES

- [1] P. Vaidyanathan, *Multirate Systems and Filter Banks*. Englewood Cliffs, NJ: Prentice Hall, 1992.
- [2] J. Woods, Ed., *Subband Image Coding*. Norwell, MA: Kluwer, 1991.
- [3] I. Daubechies, "Orthonormal bases of compactly supported wavelets," *Commun. Pure Appl. Math.*, vol. 41, pp. 909–996, Nov. 1988.
- [4] S. Mallat, "Multifrequency channel decompositions of images and wavelet models," *IEEE Trans. Acoust., Speech, Signal Processing*, vol. 37, pp. 2091–2110, Dec. 1989.
- [5] M. Vetterli and J. Kovačević, *Wavelets and Subband Coding*. Englewood Cliffs, NJ: Prentice-Hall, 1995.
- [6] O. Rioul, "A discrete-time multiresolution theory," *IEEE Trans. Signal Processing*, vol. 41, pp. 2591–2606, Aug. 1993.
- [7] R. Bamberger and M. Smith, "A filter bank for the directional decomposition of images: Theory and design," *IEEE Trans. Signal Processing*, vol. 40, pp. 882–893, Apr. 1992.
- [8] S. Basu and C. Chiang, "A complete parametrization of 2D nonseparable orthonormal wavelets," in *Proc. IEEE-SP Int. Symp. Time-Frequency Time-Scale Analysis*, Victoria, British Columbia, Canada, Oct. 1992, pp. 55–58.
- [9] T. Chen and P. Vaidyanathan, "Multidimensional multirate filters and filter banks derived from one-dimensional filters," *IEEE Trans. Signal Processing*, vol. 41, pp. 1749–1765, May 1993.
- [10] A. Cohen and I. Daubechies, "Non-separable bidimensional wavelet bases," *Rev. Mat. Iberoamericana*, vol. 9, no. 1, pp. 51–138, 1993.
- [11] G. Karlsson and M. Vetterli, "Theory of two-dimensional multirate filter banks," *IEEE Trans. Acoust., Speech, Signal Processing*, vol. 38, pp. 925–937, June 1990.
- [12] J. Kovačević and M. Vetterli, "Non-separable multidimensional perfect reconstruction filter banks and wavelet bases for  $\mathcal{R}^n$ ," *IEEE Trans. Inform. Theory*, vol. 38, pp. 533–555, Mar. 1992.
- [13] I. Shah and A. Kalker, "Algebraic theory of multidimensional filter banks and their design," *IEEE Trans. Signal Processing*, preprint.
- [14] D. Tay and N. Kingsbury, "Flexible design of multidimensional perfect reconstruction FIR 2-band filters using transformations of variables," *IEEE Trans. Image Processing*, vol. 2, pp. 466–480, Oct. 1993.
- [15] S. Venkataraman and B. Levy, "State space representations of 2-D FIR lossless transfer matrices," *IEEE Trans. Circuits Syst. II: Analog and Digital Signal Processing*, vol. 41, no. 2, pp. 117–132, Feb. 1994, to appear.
- [16] L. Villemoes, "Regularity of two-scale difference equations and wavelets," Ph.D. thesis, Mathematical Inst., Technical Univ. of Denmark, 1992.
- [17] E. Viscito and J. Allebach, "The analysis and design of multidimensional FIR perfect reconstruction filter banks for arbitrary sampling lattices," *IEEE Trans. Circuits Syst. [Video Technol.]*, vol. 38, pp. 29–42, Jan. 1991.
- [18] M. Vetterli and C. Herley, "Wavelets and filter banks: Theory and design," *IEEE Trans. Signal Processing*, vol. 40, pp. 2207–2232, Sept. 1992.
- [19] G. Karlsson, M. Vetterli, and J. Kovačević, "Non-separable two-dimensional perfect reconstruction filter banks," in *Proc. SPIE Conf. Vis. Commun. Image Processing*, Cambridge, MA, Nov. 1988, pp. 187–199.
- [20] A. Soman, P. Vaidyanathan, and T. Nguyen, "Linear phase paraunitary filter banks: Theory, factorizations and applications," *IEEE Trans. Signal Processing*, vol. 41, pp. 3480–3496, Dec. 1993.
- [21] R. Gopinath, "Wavelet transforms and time-scale analysis of signals," Master's thesis, Rice University, Houston, TX, 1990.
- [22] J. Kovačević and M. Vetterli, "FCO sampling of digital video using perfect reconstruction filter banks," *IEEE Trans. Image Processing*, vol. 2, pp. 118–122, Jan. 1993.

## Non-Wiener Solutions for the LMS Algorithm—A Time Domain Approach

N. J. Bershad and P. L. Feintuch

**Abstract**—A time domain analysis of the LMS algorithm is presented for a sinusoidal deterministic reference input. For the sinusoidal reference input only, the  $N$ -dimensional time-varying linear matrix recursion for the weight vector is solved using a 2-D orthogonal subspace decomposition. Using this weight vector solution, it is shown that there exists a linear time-invariant relationship between the desired input and the filter output.

#### I. INTRODUCTION

The LMS adaptive filter algorithm is usually comprised of a tapped delay line with uniform tap spacing; a set of adjustable weights that multiply the tap outputs, and a summer [2]. The weights are adjusted recursively, based on the difference between the output of the summer and an external desired signal. When the algorithm input is deterministic, the behavior of the algorithm is often quite different than when the input is a stochastic process [1], [3]. These cases are denoted non-Wiener solutions to the algorithm. This behavior was studied for adaptive noise cancelling when the reference input was a deterministic sine wave [1] and for a noise corrupted sine wave reference when the desired signal is either a sine wave or white noise in [3]. The analysis in [1] was based on an approximation that led to a time-invariant transfer function between the algorithm error and the adaptive filter output (although the adaptive filter weights are time varying even in steady state). This allowed the authors to apply  $Z$  transforms to the adaptive loop and to find an equivalent steady-state transfer function. Shensa [3] studied the case when the reference was a deterministic sine wave in white noise. Conolly and Su [4] studied the noiseless problem for a two-tap filter using a state-space approach and obtained an exact closed-form solution. The solution was based on finding a time-invariant state equation for the two-tap weights. This work leads to a simple understanding of non-Wiener-type adaptation but is not applicable to adaptive filters with more than two taps.

This correspondence studies the same problem as in [1] but uses a time-domain analysis of the adaptive filter behavior to obtain results. In contrast to [1], where loop time-invariant system arguments were used, an orthogonal decomposition approach yields results in a

Manuscript received October 19, 1993; revised October 16, 1994. This work was supported by Hughes Aircraft Company, Fullerton, CA, a subsidiary of General Motors Hughes Electronics. The associate editor coordinating the review of this paper and approving it for publication was Dr. Fuyun Ling.

N. J. Bershad is with the Electrical and Computer Engineering Department, University of California, Irvine, CA 92717 USA. He is also a Consultant with Hughes Aircraft Company, Fullerton, CA USA.

P. L. Feintuch is with the Undersea Systems Division, Hughes Aircraft Company, Fullerton, CA USA

IEEE Log Number 9410310.